Electronic Supplementary Material (ESI) for Journal of Materials Chemistry A.

Supporting Information for

The heterostructure CoFe@($Co_{0.5}Fe_{0.5}$)S@NCNT anchored on the rice husk-based hierarchical porous carbon as a bifunctional cathode catalyst for Zn-air batteries

Jin Yang[a], Jun Shi[b], Yupeng Wu[a], Huimin Liu[a], Zhiqiang Liu[a], Qinwen You[a], Xinxin Li[a], Linchuan Cong[a], Debo Liu[a], Fangbing Liu[a], Yue Jiang[d], Nan Lin[*a], Wenli Zhang[c,e], Haibo Lin[a]

[a] *State Key Laboratory of Inorganic Synthesis and Preparative Chemistry, College of Chemistry, Jilin University, Changchun 130012, China*

[b] *School of Chemical Engineering & New Energy Materials, Zhuhai College of Science and Technology, Zhuhai 519041, China*

[c] *Guangdong Provincial Key Laboratory of Plant Resources Biorefinery, School of Chemical Engineering & Light Industry, Guangdong University of Technology GDUT, Guangzhou 510006, China*

[d] *Key Laboratory of Bionic Engineering of Ministry of Education, College of Biological and Agricultural Engineering, Jilin University, Changchun 130025, China*

[e] *Guangdong Provincial Laboratory of Chemistry and Fine Chemical Engineering Jieyang Center, Jieyang 515200, China*

* Corresponding authors: nanlin@jlu.edu.cn (Nan Lin[*a])

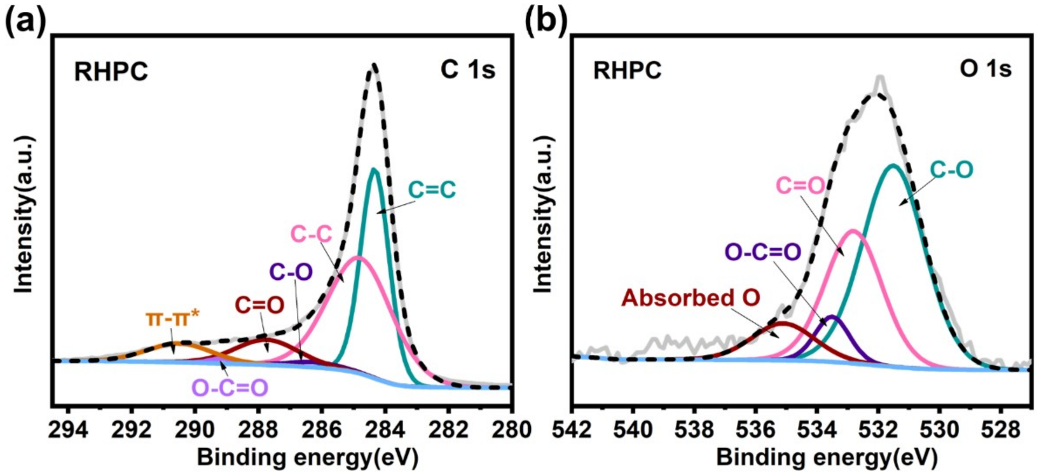

Fig. S1 High-resolution XPS spectra of RHPC for (a) C 1s and (b) O 1s.

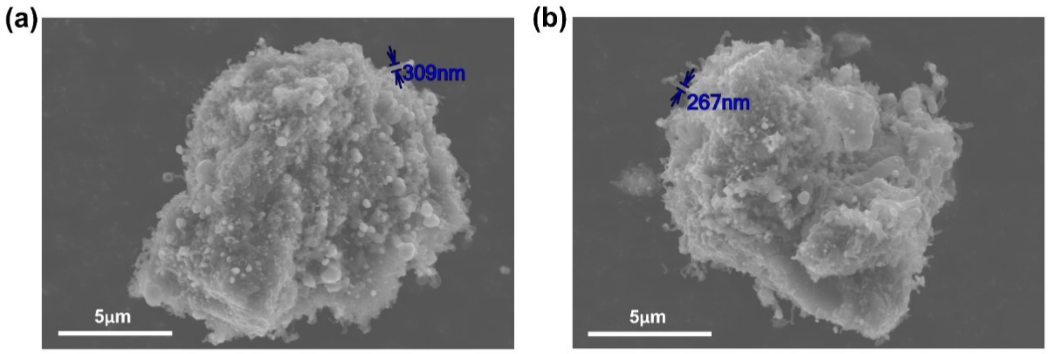

Fig. S2 SEM images of (a) CoFe@NC and (b) $(Co_{0.5}Fe_{0.5})S$@NC.

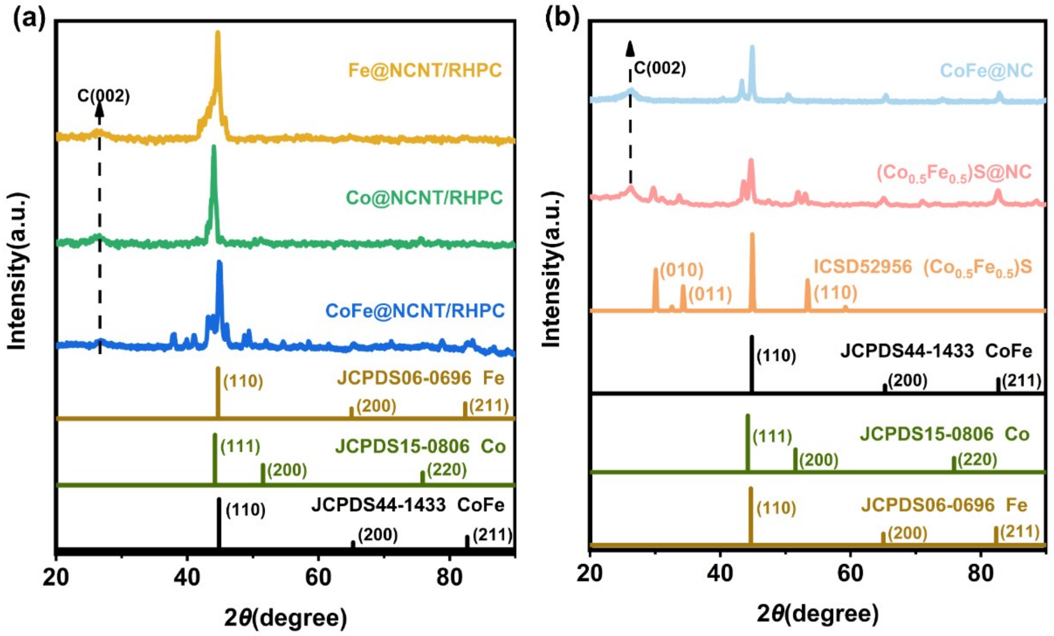

Fig. S3 (a) XRD of Fe@NCNT/RHPC, Co@NCNT/RHPC and CoFe@NCNT/RHPC; (b) XRD of CoFe@NC and $(Co_{0.5}Fe_{0.5})S$@NC.

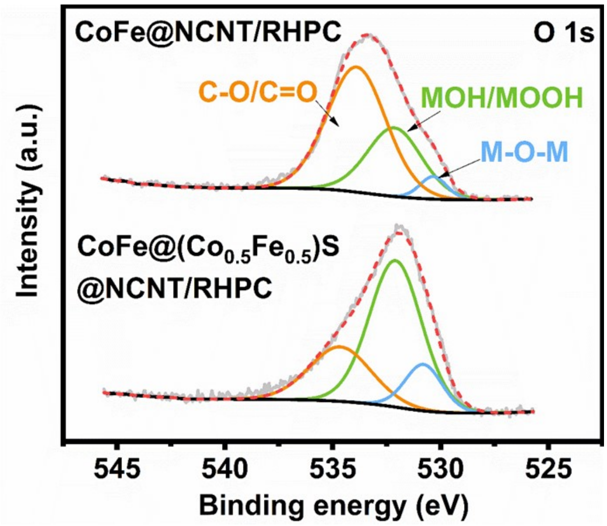

Fig. S4 High-resolution XPS spectra of CoFe@NCNT/RHPC and CoFe@$(Co_{0.5}Fe_{0.5})S$@NCNT/RHPC for O 1s.

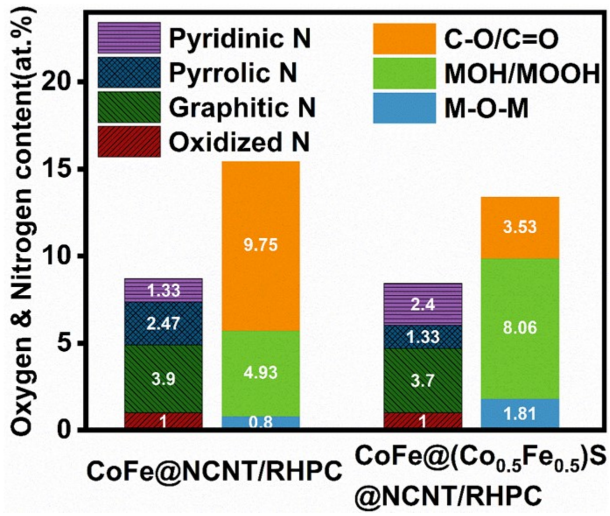

Fig. S5 The contents of various doped N and various doped O of CoFe@NCNT/RHPC and CoFe@$(Co_{0.5}Fe_{0.5})S$@NCNT/RHPC.

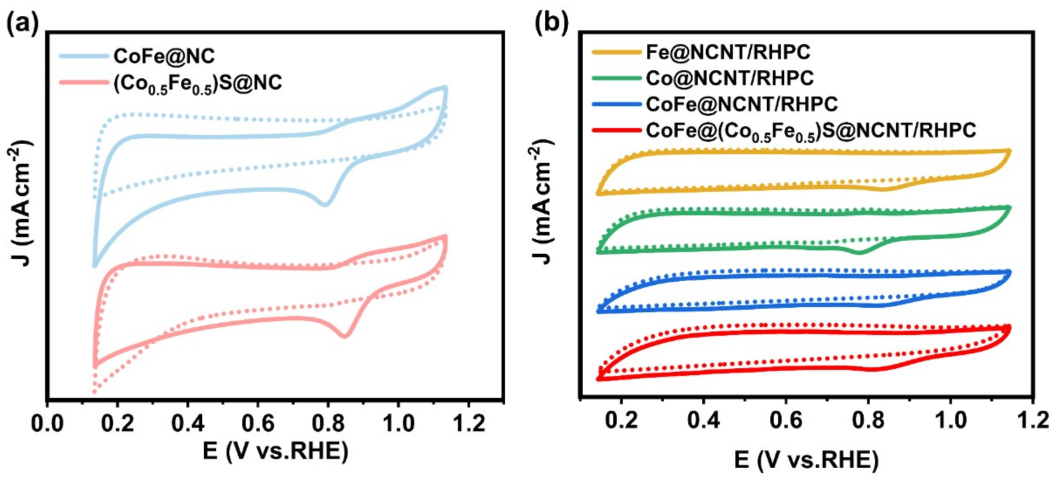

Fig. S6 CV curves of prepared catalysts in (a) O_2-saturated and (b) N_2-saturated 0.1 M KOH at a scan rate of 50 mV s^{-1}.

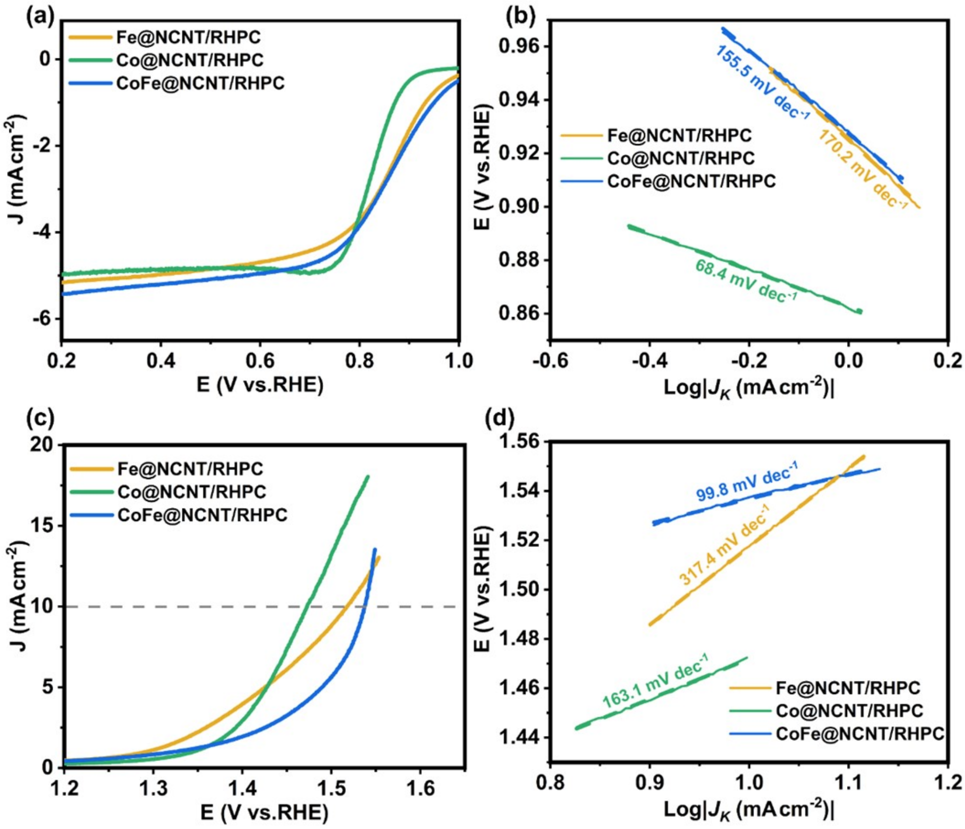

Fig. S7 (a) LSV polarization curves for ORR at a rotation speed of 1600 rpm in O_2-saturated 0.1 M KOH with a scan rate of 5 mV s^{-1}, (b) Tafel slopes, (c) LSV polarization curves for OER with a scan rate of 5 mV s^{-1}, (d) Tafel slopes for Fe@NCNT/RHPC, Co@NCNT/RHPC and CoFe@NCNT/RHPC.

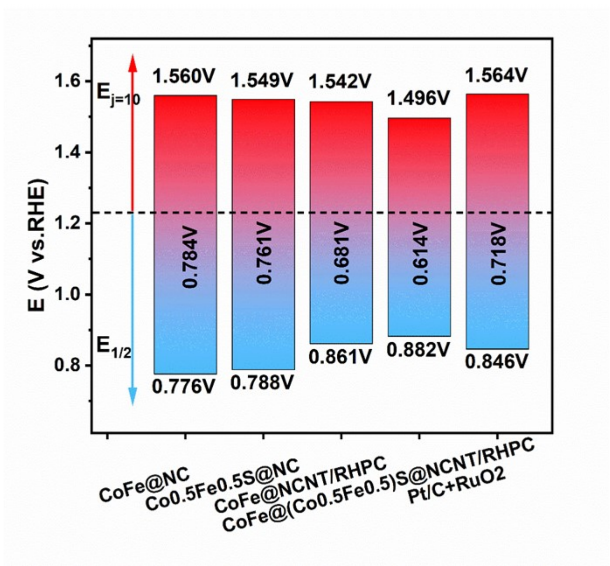

Fig. S8 Potential gaps patterns.

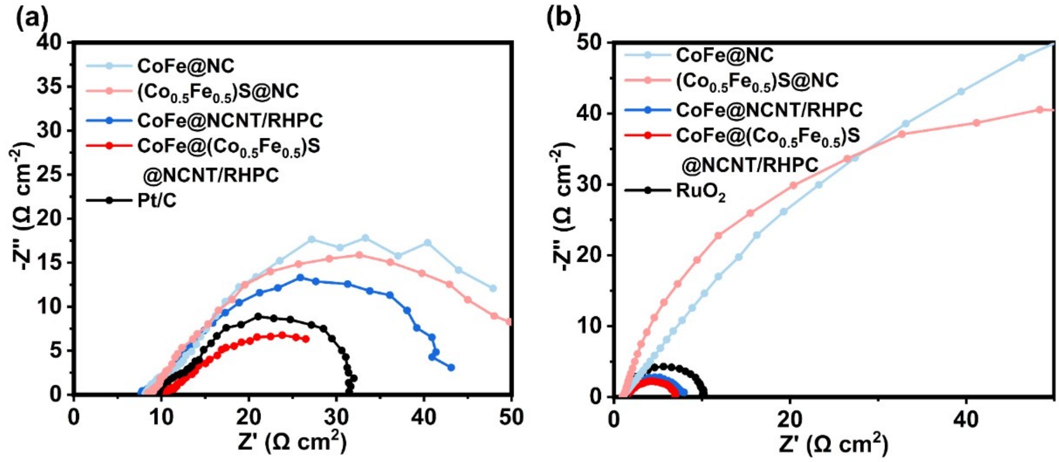

Fig. S9 (a) EIS spectra of CoFe@NC, $(Co_{0.5}Fe_{0.5})S$@NC, CoFe@NCNT/RHPC, CoFe@$(Co_{0.5}Fe_{0.5})S$@NCNT/RHPC and Pt/C in O_2-saturated 0.1 M KOH; (b) EIS spectra of CoFe@NC, $(Co_{0.5}Fe_{0.5})S$@NC, CoFe@NCNT/RHPC, CoFe@$(Co_{0.5}Fe_{0.5})S$@NCNT/RHPC and RuO_2 in 1 M KOH.

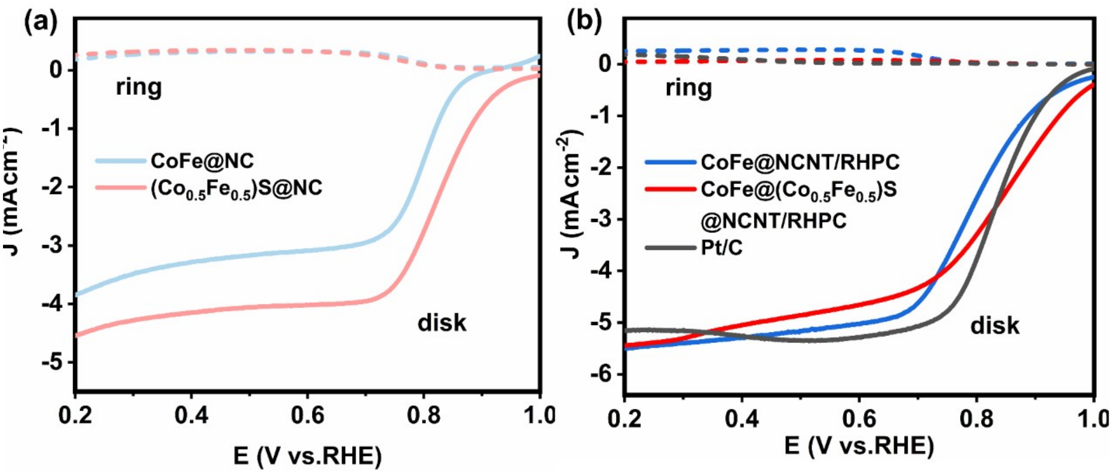

Fig. S10 LSV curves of CoFe@NC, $(Co_{0.5}Fe_{0.5})S$@NC, CoFe@NCNT/RHPC, CoFe@$(Co_{0.5}Fe_{0.5})S$@NCNT/RHPC and Pt/C using RRDE scanned in O_2-saturated 0.1 M KOH aqueous electrolyte at a rotation speed of 1600 rpm.

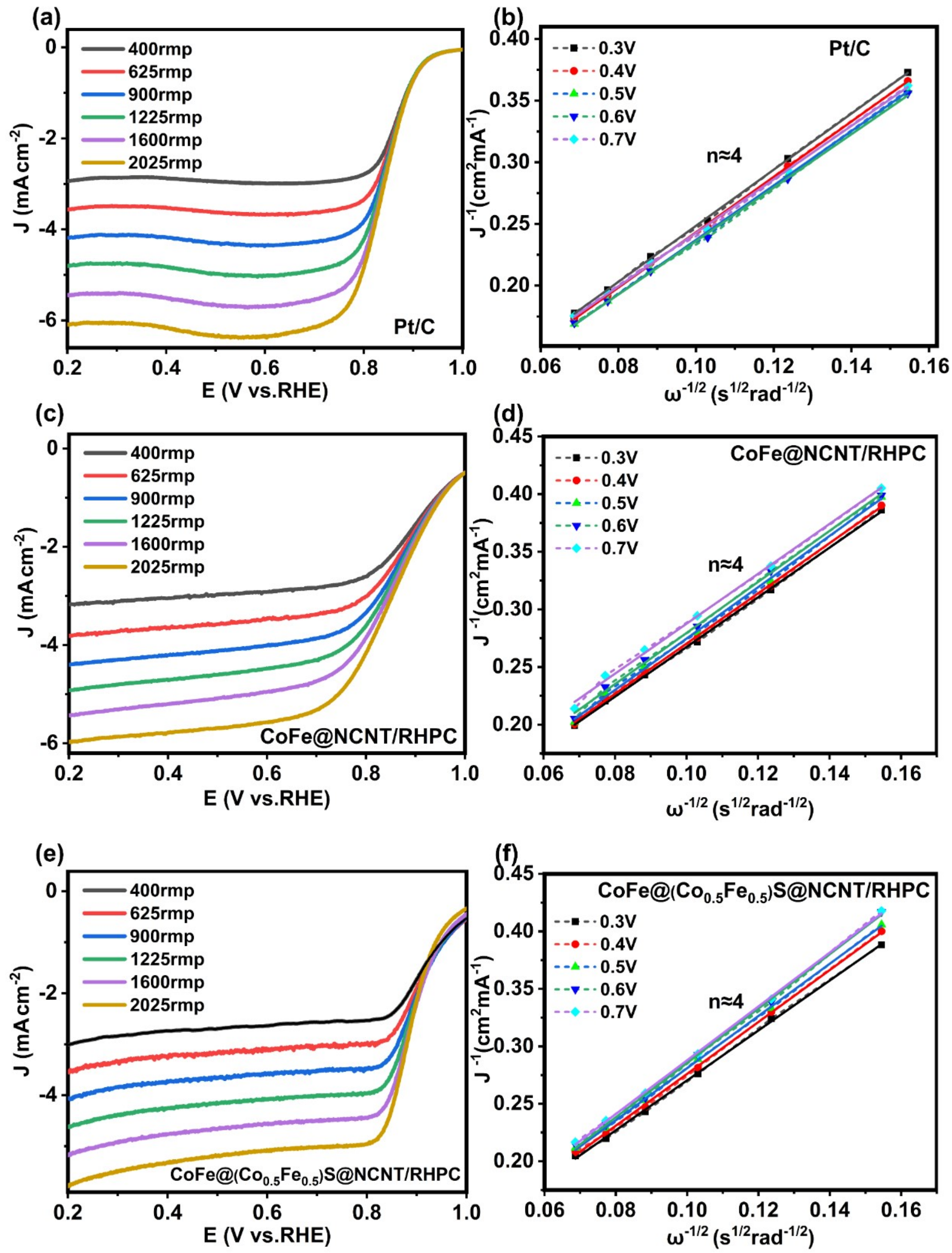

Fig. S11 (a, c, e) LSV curves of Pt/C, CoFe@NCNT/RHPC, CoFe@($Co_{0.5}Fe_{0.5}$)S@NCNT/RHPC at different rotating speeds; (b, d, f) shows the corresponding K-L plots at different potentials including the calculated number of electron transfer (n) per O_2.

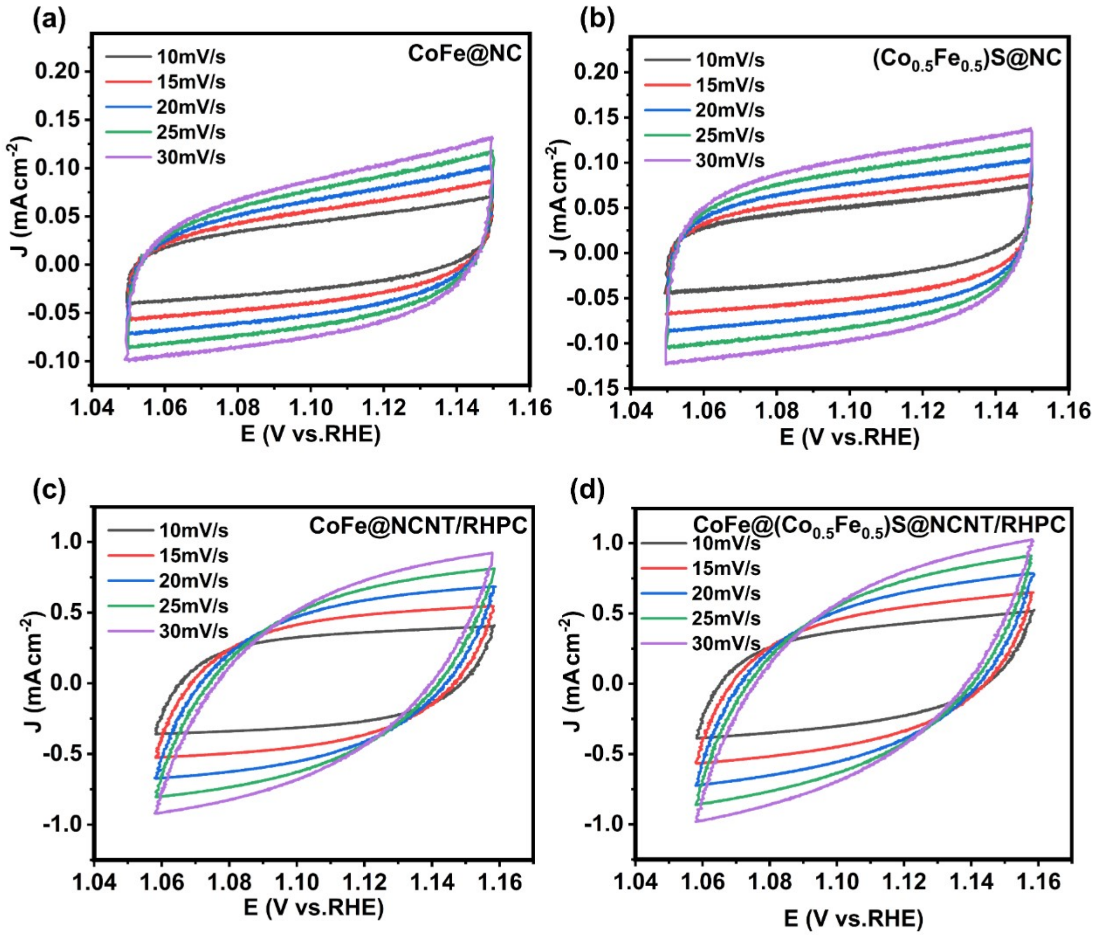

Fig. S12 Cyclic voltammetry curves at different scanning rates (from 10 to 30 mV s^{-1}) of (a) CoFe@NC, (b) $(Co_{0.5}Fe_{0.5})S$@NC, (c) CoFe@NCNT/RHPC, (d) CoFe@$(Co_{0.5}Fe_{0.5})S$@NCNT/RHPC in N_2-saturated 0.1 M KOH.

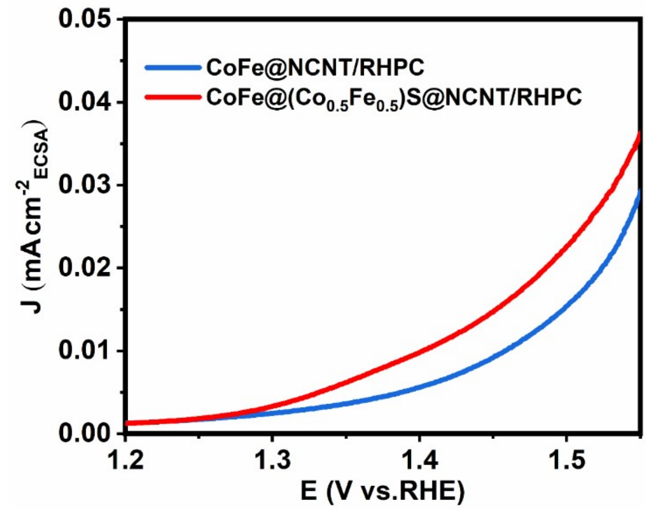

Fig. S13 OER polarization curves normalized by ESCA.

ECSA is obtained by C_{dl}：ECSA = C_{dl}/C_s,[1] C_s = 0.040 mF cm^{-2}

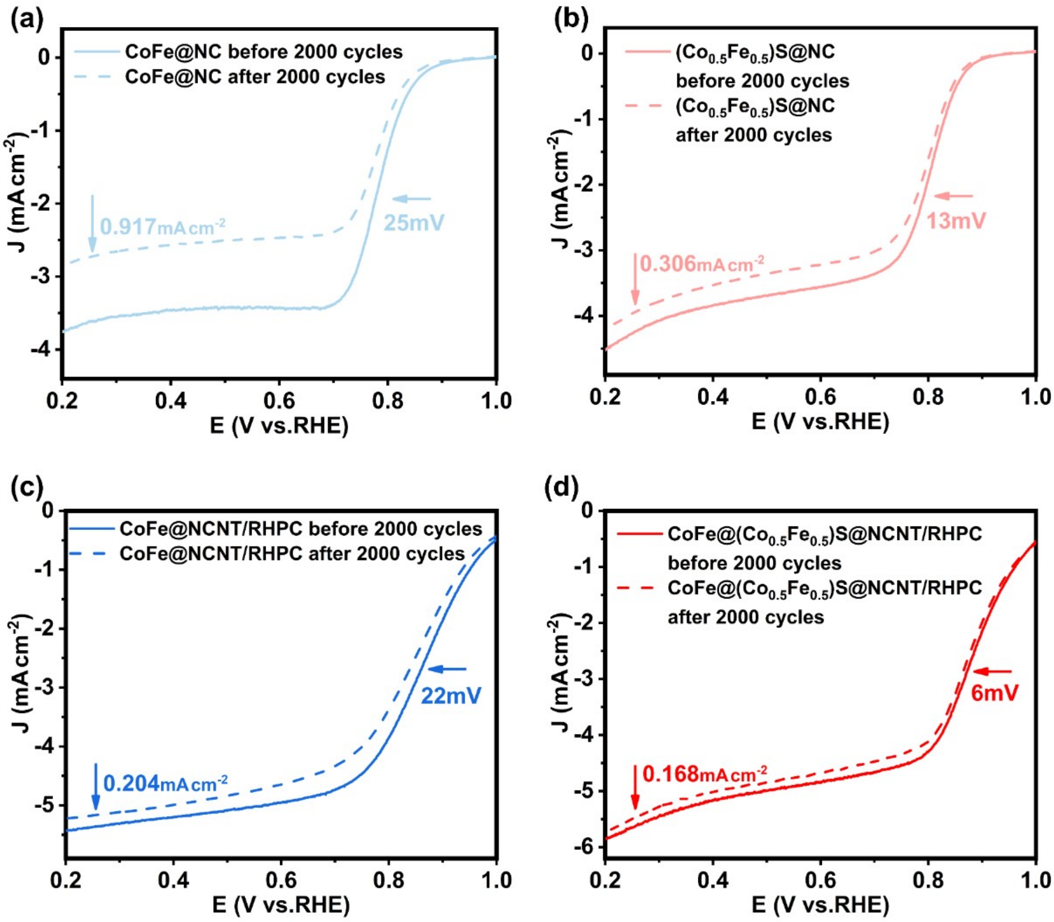

Fig. S14 ORR polarization curves of (a) CoFe@NC, (b) $(Co_{0.5}Fe_{0.5})S$@NC, (c) CoFe@NCNT/RHPC, (d) CoFe@$(Co_{0.5}Fe_{0.5})S$@NCNT/RHPC before and after 2000 cycles in 0.1M KOH.

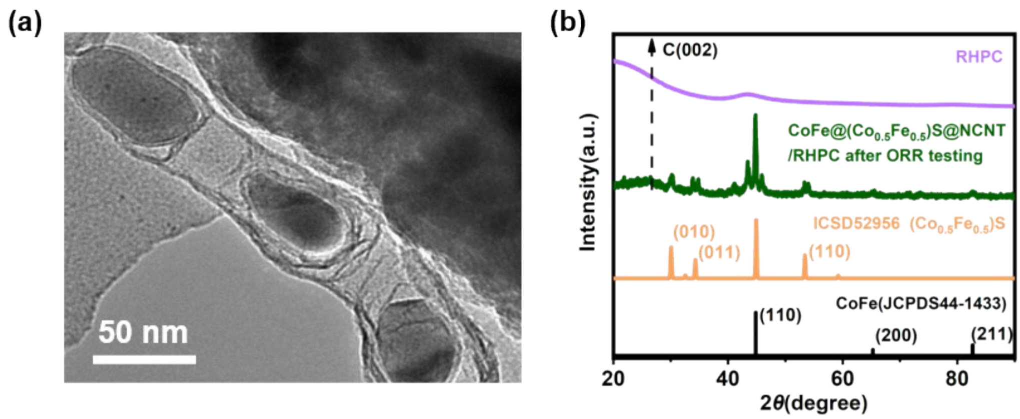

Fig. S15 (a) TEM image and (b) XRD pattern of CoFe@$(Co_{0.5}Fe_{0.5})S$@NCNT/RHPC after the ORR testing in 0.1 M KOH aqueous solution.

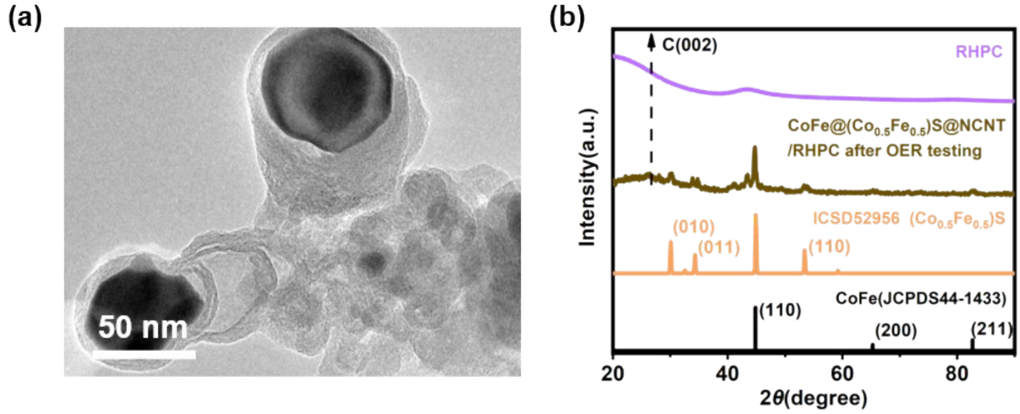

Fig. S16 (a) TEM image and (b) XRD pattern of CoFe@($Co_{0.5}Fe_{0.5}$)S@NCNT/RHPC after OER testing in 1 M KOH aqueous solution.

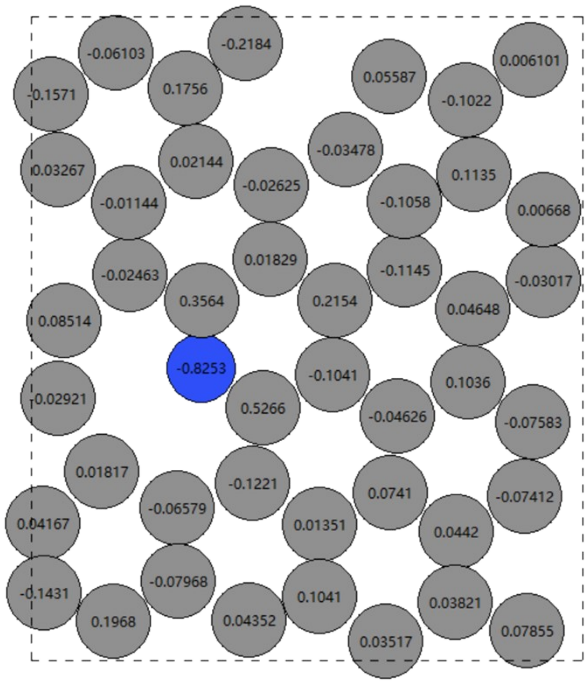

Fig. S17 The atomic charge (the numbers) of NCNT.

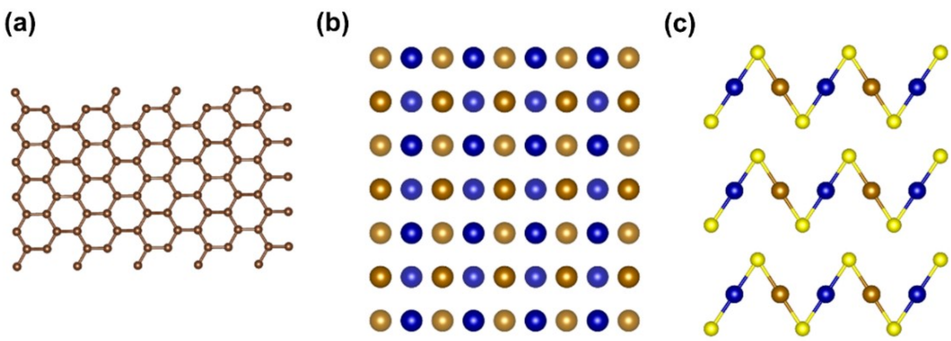

Fig. S18 Models for (a) C(001), (b) CoFe(110), (c) ($Co_{0.5}Fe_{0.5}$)S(110).

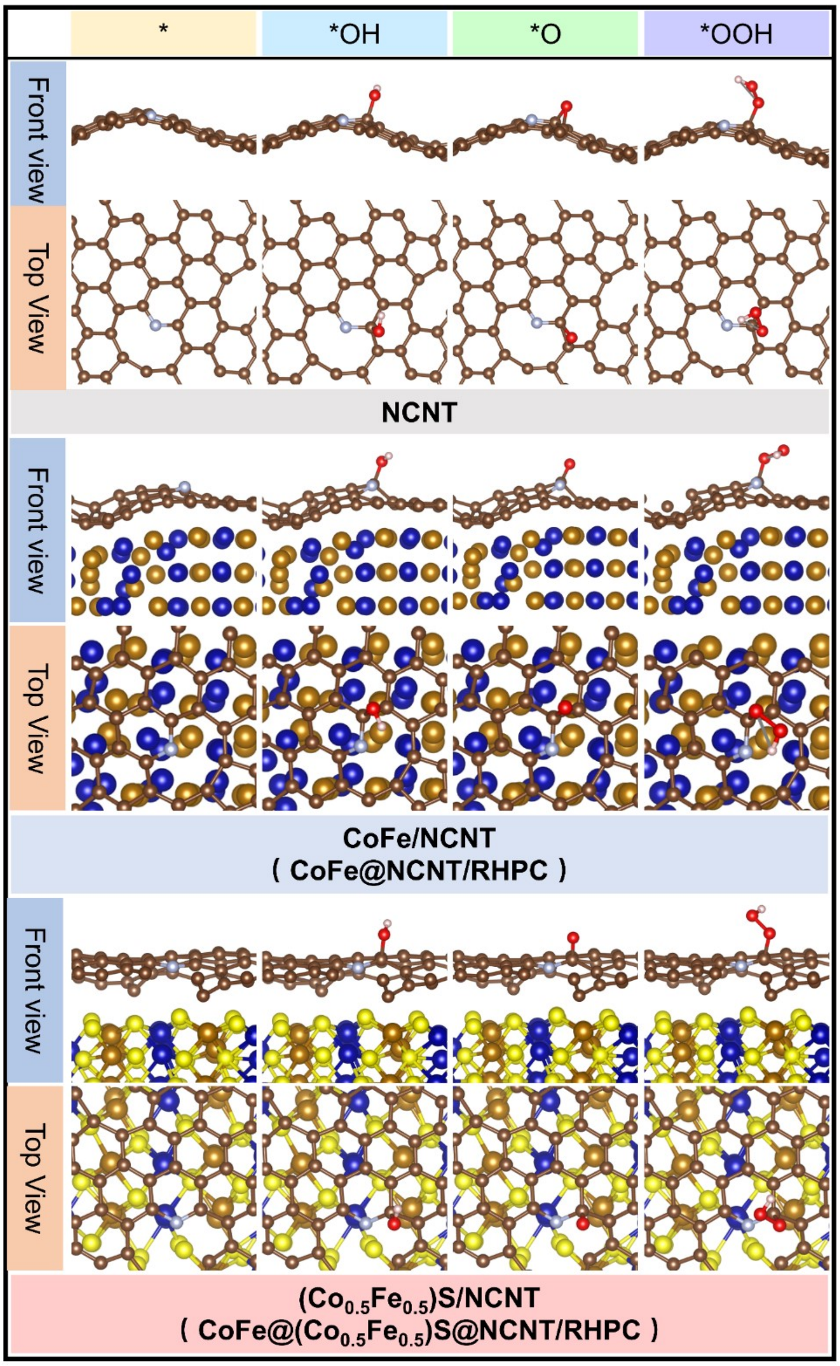

Fig. S19 DFT optimized ORR/OER intermediate structures on C sites for NCNT, CoFe/NCNT(CoFe@NCNT/RHPC) and $(Co_{0.5}Fe_{0.5})S$/NCNT(CoFe@$(Co_{0.5}Fe_{0.5})S$@NCNT/RHPC).

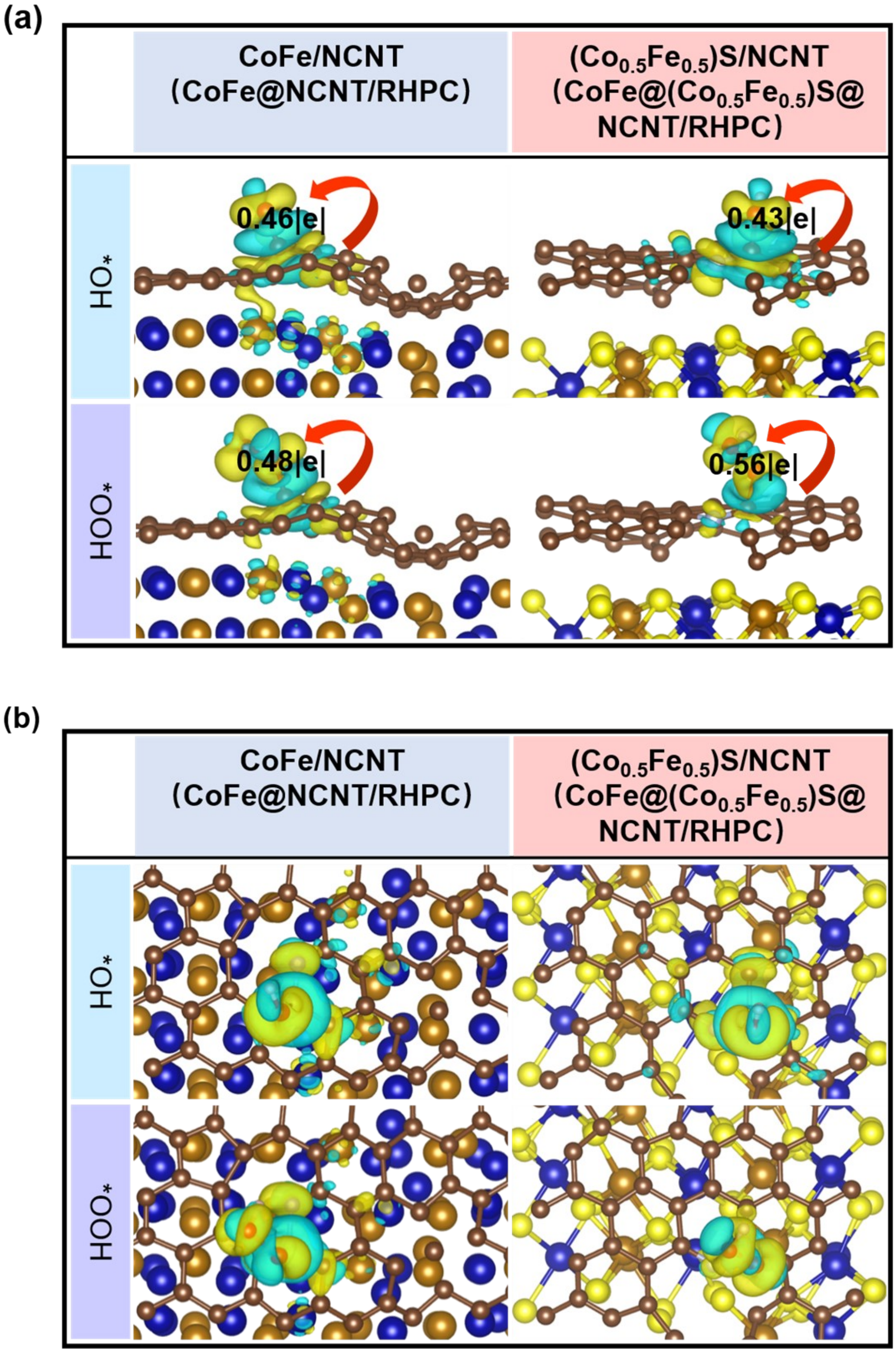

Fig. S20 (a) Front view and (b) top view of differential electron density and bader charge of CoFe/NCNT(CoFe@NCNT/RHPC) and $(Co_{0.5}Fe_{0.5})S$/NCNT(CoFe@$(Co_{0.5}Fe_{0.5})S$@NCNT/RHPC) structures during adsorption of the intermediates (*OH and *OOH).

Tab. S1 Specific surface area, pore volume, and pore size of RHPC, CoFe@NC,

$(Co_{0.5}Fe_{0.5})S$@NC, CoFe@NCNT/RHPC and CoFe@$(Co_{0.5}Fe_{0.5})S$@NCNT/RHPC.

Samples	Specific surface area (m^2g^{-1})	Micro pores volume (mLg^{-1})	Meso pores volume (mLg^{-1})	Total pores volume (mLg^{-1})	Average pore size (nm)
RHPC	2266.3	0.88	0.52	1.40	0.80
CoFe@NC	71.0	0.02	0.09	0.11	1.12
$(Co_{0.5}Fe_{0.5})S$@NC	29.1	0.02	0.04	0.06	1.35
CoFe@NCNT/RHPC	495.4	0.17	0.30	0.47	0.76
CoFe@$(Co_{0.5}Fe_{0.5})S$@NCNT/RHPC	510.2	0.18	0.32	0.50	0.74

Tab. S2 The atomic composition of RHPC, CoFe@NCNT/RHPC and CoFe@$(Co_{0.5}Fe_{0.5})S$@NCNT/RHPC obtained from XPS spectra.

Samples	C 1s (At.%)	N 1s (At.%)	S 2p (At.%)	O 1s (At.%)	Fe 2p (At.%)	Co 2p (At.%)
RHPC	96.39	0.86		2.75		
CoFe@NCNT/RHPC	83.90	7.26	0.18	7.60	0.41	0.66
CoFe@$(Co_{0.5}Fe_{0.5})S$@NCNT/RHPC	81.98	7.57	1.57	7.27	0.69	0.93

Tab. S3 Summary of the ORR/OER bifunctional performance of transition metal-based electrocatalysts reported recently.

Catalyst	$E_{1/2}$ (vs. RHE)	$E_{j=10}$ (vs. RHE)	ΔE (V)	Ref.
CoFe@($Co_{0.5}Fe_{0.5}$)S@NCNT/RHPC	0.882	1.496	0.614	This work
CoFe@NCNT/RHPC	0.861	1.542	0.681	This work
CoFe@NCS-24	0.88	1.57	0.69	[2]
Fe,Co,N–C	0.90	1.64	0.74	[3]
FeCoMoS@NG	0.83	1.468	0.638	[4]
HHPC	0.78	1.58	0.80	[5]
e-N/P-C-700	0.867	1.66	0.76	[6]
NCo_3O_4@NC-2	0.77	1.50	0.78	[7]
Co@hNCTs-800	0.87	1.63	0.76	[8]
Fe/Co-N/S-Cs	0.835	1.515	0.680	[9]
$Ni_{0.5}Fe_{0.5}$@NCNTs	0.84	1.5	0.660	[10]
FeNiNCNT/NCS	0.84	1.59	0.75	[11]
$Fe_8Co_{0.2}$-NC-800	0.820	1.632	0.812	[12]
Fe-N_X@NSCST-ZL	0.92	1.71	0.79	[13]
CoS/Fe3S4@SNCP	0.85	1.50	0.65	[14]
SA-Fe-SNC@900	0.876	1.632	0.756	[15]
Fe–SAs@N/S-PCSs	0.90	1.68	0.78	[16]
Fe–N/S-CNT–GR	0.91	1.60	0.69	[17]
$Fe_xCo_{9-x}S_8$-NHCS-V	0.80	1.53	0.73	[18]
CoFe/S-N-C	0.855	1.588	0.733	[19]
FeCo-NCNTs	0.90	1.55	0.65	[20]
PB@ Met-700	0.855	1.56	0.705	[21]

Tab. S4 EIS calculation parameters of all samples for ORR in 0.1 M KOH.

	CoFe@NC	($Co_{0.5}Fe_{0.5}$)S@NC	CoFe@NCNT/RHPC	CoFe@($Co_{0.5}Fe_{0.5}$)S@NCNT/RHPC	Pt/C
R_S(Ωcm^{-2})	8.50	8.88	8.19	10.59	9.57
R_H(Ωcm^{-2})	4.68	3.69	3.50	3.46	3.65
R_L(Ωcm^{-2})	35.84	33.68	28.67	13.64	18.37
C_H($F\ cm^{-2}$)	0.001	0.021	0.007	0.008	0.004
C_L($F\ cm^{-2}$)	0.009	0.060	0.052	0.075	0.032

Tab. S5 EIS calculation parameters of all samples for OER in 1 M KOH.

	CoFe@NC	($Co_{0.5}Fe_{0.5}$)S@NC	CoFe@NCNT/RHPC	CoFe@($Co_{0.5}Fe_{0.5}$)S@NC	RuO_2

				NT/RHPC	
R_S(Ωcm^{-2})	0.96	0.99	1.11	1.26	1.21
Rct(Ωcm^{-2})	232.80	103.20	7.34	6.15	9.17
Yo(S sec^n cm^{-2})	0.004	0.008	0.060	0.040	0.002
n	0.683	0.860	0.769	0.744	0.935

Tab. S6 Charge and discharge voltages and efficiencies of Zinc–air battery with CoFe@($Co_{0.5}Fe_{0.5}$)S@NCNT/RHPC at different turn numbers.

Number of battery cycles	100	200	400	600	800
Discharge voltage (V)	1.12	1.12	1.13	1.08	1.03
Charge voltage (V)	2.10	2.09	2.10	2.09	2.12
Charge and discharge efficiency (%)	53.2	53.8	53.8	51.6	48.5

Tab. S7 Comparisons of liquid rechargeable Zn-air batteries performances for state-of-the-art catalysts.

Catalyst	Maximum power density (mW cm^{-2})	Catalyst Loading (mg cm^{-2})	Cycling Stability @ 5 mA cm^{-2} (min)	Cycling Stability @ 10 mA cm^{-2} (min)	Specific capacity (mAh g^{-1}) @ 10 mA cm^{-2}	Ref.
CoFe@($Co_{0.5}Fe_{0.5}$)S@NCNT/RHPC	136	1		10000	813.6	This work
Fe/Co-N/S-Cs	102.63	1	1600			[9]
FeNi@NCNT/NCS	103	1			687.4	[11]
$Fe_8Co_{0.2}$-NC-800	124.9	1.14	18660		704	[12]
Fe-N_X@NSCST-ZL					778	[13]
SA-Fe-SNC@900	218.6	2	9600		798.7	[15]
Fe–N/S-CNT–GR	123	1		18000	912	[17]
CoFe/S-N-C	120	1		6000	814	[19]
PB@ Met-700	148	2		5400	781	[21]
FeCo-NSC	152.8	2		7200	782.1	[22]
FeSA-FeNC@NSC	259.88			6000	811.03	[23]
MIL/ZIF-4-700 °C-NH_3	176.3	2		30000	893.5	[24]
NSCA/FeCo	132	1		5000	804.5	[25]

γ-Fe_2O_3@CNFs-12	99.06	1			661.6	26
FeNi-NCS-2	109.8	1		1000	639.71	27
Co@N-HPCF-800	136.2	1	3000		723	28
Ni SAs-NC	172	2		18000		29
FeSA-S/N-C	128.35	0.6	30000		800.92	30
CoP@NC-Ru	175	1.5	3000		780	31
$NiFeO_x$@VACNTs	194	3.5	90000		800	32
Fe/Fe_3C@$Fe\text{-}N_{x\text{-}C}$	147	1	12000			33
3D SAFe	156	0.48		4800	815	34
FeNCFs-x	173	1		9900	717	35
CoFe@HNSs	131.3	0.5	8400			36
FeNC-900-8	124.9	1			816.4	37
FeCo-N-C	196.3	2		4620	728.6	38
SA-Fe-3DOMC	140	2			786.6	39
Fe-NP/MNCF	111.6	1		10800	794.8	40
POP-Fe/Ni-900	256	1.25	7200		740	41
Fe-SAs/S,N-C/rGO	127.36		37200		817.23	42

Tab. S8 Gibbs free energy change (ΔG) of NCNT, CoFe/NCNT(CoFe@NCNT/RHPC) and $(Co_{0.5}Fe_{0.5})S$/NCNT(CoFe@$(Co_{0.5}Fe_{0.5})S$@NCNT/RHPC) at different potentials during OER.

ΔG (eV)	**U = 0 V**			**U = 1.23 V**		
	NCNT	CoFe/NCNT	$(Co_{0.5}Fe_{0.5})S$/ NCNT	NCNT	CoFe/NCNT	$(Co_{0.5}Fe_{0.5})S$/ NCNT
Step 1	1.460	0.475	1.331	0.230	-0.755	0.101
Step 2	-0.215	0.491	0.654	-1.445	-0.739	-0.576
Step 3	1.290	1.798	1.388	0.060	0.568	0.158
Step 4	2.385	2.156	1.548	1.155	0.926	0.318

Tab. S9 The bond length parameters of C-O, O-O and O-H of CoFe/NCNT(CoFe@NCNT/RHPC)

Bond length(Å)	CoFe/NCNT-OH	$(Co_{0.5}Fe_{0.5})S$/NCNT-OH	CoFe/NCNT-OOH	$(Co_{0.5}Fe_{0.5})S$/NCNT-OOH
C-O	1.45	1.48	1.47	1.54
O-O	-	-	1.47	1.46
O-H	0.98	0.98	0.99	0.98

and $(Co_{0.5}Fe_{0.5})S$/NCNT(CoFe@$(Co_{0.5}Fe_{0.5})S$@NCNT/RHPC) absorbed *OH and *OOH.

Reference

1 A. Roy, A. Ray, S. Saha, M. Ghosh, T. Das, M. Nandi, G. Lal, S. Das, *Int. J. Energy*

Res., 2021, **45**, 16908.
2 H. Cheng, Y. Zhuang, C. Meng, B. Chen, J. Chen, A. Yuan, H. Zhou, *Appl. Surf. Sci.*, 2023, **607**, 154953.
3 S. Sarkar, A. Biswas, E. E. Siddharthan, R. Thapa, R. S. Dey, *ACS Nano*, 2022, **16**, 7890.
4 S. Ramakrishnan, J. Balamurugan, M. Vinothkannan, A. R. Kim, S. Sengodan, D. J. Yoo, *Appl. Catal., B*, 2020, **279**, 119381.
5 X. Xiao, X. Li, Z. Wang, G. Yan, H. Guo, Q. Hu, L. Li, Y. Liu, J. Wang, *Appl. Catal., B*, 2020, **265**, 118603.
6 K. Yuan, D. Lützenkirchen-Hecht, L. Li, L. Shuai, Y. Li, R. Cao, M. Qiu, X. Zhuang, M. K. H. Leung, Y. Chen, U. Scherf, *J. Am. Chem. Soc.*, 2020, **142**, 2404.
7 Z. Wang, W. Xu, X. Chen, Y. Peng, Y. Song, C. Lv, H. Liu, J. Sun, D. Yuan, X. Li, X. Guo, D. Yang, L. Zhang, *Adv. Funct. Mater.*, 2019, **29**, 1902875.
8 Q. Zhou, Z. Zhang, J. Cai, B. Liu, Y. Zhang, X. Gong, X. Sui, A. Yu, L. Zhao, Z. Wang, Z. Chen, *Nano Energy*, 2020, **71**, 104592.
9 C. Li, H. Liu, Z. Yu, *Appl. Catal., B*, 2019, **241**, 95.
10 C. Sun, Y.-J. Zhao, X.-Y. Yuan, J.-B. Li, H.-B. Jin, *Rare Metals*, 2022, **41**, 2616.
11 J.-T. Ren, L. Chen, Y.-S. Wang, W.-W. Tian, L.-J. Gao, Z.-Y. Yuan, *ACS Sustain. Chem. Eng.*, 2020, **8**, 223.
12 T. Jin, J. Nie, M. Dong, B. Chen, J. Nie, G. Ma, *Nano-micro Lett.*, 2022, **15**, 26.
13 C. Li, Y. Zhang, M. Yuan, Y. Liu, H. Lan, Z. Li, K. Liu, L. Wang, *Chem. Eng. J.*, 2023, **471**, 144515.
14 L. Yan, B. B. Xie, C. Yang, Y. H. Wang, J. Q. Ning, Y. J. Zhong, Y. Hu, *Adv. Energy Mater.*, 2023, **13**, 2204245.
15 Z. H. Chen, X. W. Peng, Z. X. Chen, T. Z. Li, R. Zou, G. Shi, Y. F. Huang, P. Cui, J. Yu, Y. L. Chen, X. Chi, K. P. Loh, Z. Q. Liu, X. H. Li, L. X. Zhong, J. Lu, *Adv. Mater.*, 2023, **35**, 2209948.
16 W. Wei, F. Lu, L. Cui, Y. Zhang, Y. Wei, L. Zong, *Carbon*, 2022, **197**, 112.
17 W. Y. Noh, J. Mun, Y. Lee, E. M. Kim, Y. K. Kim, K. Y. Kim, H. Y. Jeong, J. H. Lee, H.-K. Song, G. Lee, J. S. Lee, *ACS Catal.*, 2022, **12**, 7994.
18 S.-J. Li, Y. Xie, B.-L. Lai, Y. Liang, K. Xiao, T. Ouyang, N. Li, Z.-Q. Liu, *Chin. J. Catal.*, 2022, **43**, 1502.
19 G. Li, Y. Tang, T. Fu, Y. Xiang, Z. Xiong, Y. Si, C. Guo, Z. Jiang, *Chem. Eng. J.*, 2022, **429**, 132174.
20 S. Y. Lin, L. X. Xia, L. Zhang, J. J. Feng, Y. Zhao, A. J. Wang, *Chem. Eng. J.*, 2021, **424**.
21 Y. B. Lian, K. F. Shi, H. J. Yang, H. Sun, P. W. Qi, J. Ye, W. B. Wu, Z. Deng, Y. Peng, *Small*, 2020, **16**, 1907368.
22 Y. Wu, C. Ye, L. Yu, Y. Liu, J. Huang, J. Bi, L. Xue, J. Sun, J. Yang, W. Zhang, X. Wang, P. Xiong, J. Zhu, *Energy Storage Mater.*, 2022, **45**, 805.
23 W. J. Zhai, S. H. Huang, C. B. Lu, X. N. Tang, L. B. Li, B. Y. Huang, T. Hu, K. Yuan, X. D. Zhuang, Y. W. Chen, *Small*, 2022, **18**, 2107225.
24. R. Song, L. Guan, L. Fan, X. Miao, H. Zhang, J. Cheng, T. Zhou, C. Ni and J. Fan, *J. Energy Storage*, 2024, **80**, 110345.

25. Y. Zhang, X. Zhang, Y. Li, J. Wang, S. Kawi and Q. Zhong, *Nano Res.*, 2023, **16**, 6870-6880.
26. Z. Yao, Y. Li, D. Chen, Y. Zhang, X. Bao, J. Wang and Q. Zhong, *Chem. Eng. J.*, 2021, **415**, 129033.
27. Z. Yao, D. Chen, Y. Li, Q. Lyu, J. Wang and Q. Zhong, *Int. J. Hydrogen Energy*, 2022, **47**, 984-992.
28. Y. Zhang, Q. He, Z. Chen, Y. Chi, J. Sun, D. Yuan and L. Zhang, *J. Energy Chem.*, 2023, **76**, 117-126.
29. H. Jiang, J. Xia, L. Jiao, X. Meng, P. Wang, C.-S. Lee and W. Zhang, *Appl. Catal., B*, 2022, **310**, 121352.
30. S. Zhou, C. Chen, J. Xia, L. Li, X. Qian, F. Yin, G. He, Q. Chen and H. Chen, *Small*, 2024, DOI: 10.1002/smll.202310224, e2310224-e2310224.
31. M. M. Kumar, C. Aparna, A. K. Nayak, U. V. Waghmare, D. Pradhan and C. R. Raj, *ACS Appl. Mater. Interfaces*, 2024, **16**, 3542-3551.
32. Y. Yan, Y. Xu, B. Zhao, Y. Xu, Y. Gao, G. Chen, W. Wang and B. Y. Xia, *J. Mater. Chem. A*, 2020, **8**, 5070-5077.
33. L. B. Zong, X. Chen, S. L. Liu, K. C. Fan, S. M. Dou, J. Xu, X. X. Zhao, W. J. Zhang, Y. W. Zhang, W. C. Wu, F. H. Lu, L. X. Cui, X. F. Jia, Q. Zhang, Y. Yang, J. Zhao, X. Li, Y. D. Deng, Y. N. Chen and L. Wang, *J. Energy Chem.*, 2021, **56**, 72-79.
34. T. Jin, J. Nie, M. Dong, B. Chen, J. Nie and G. Ma, *Nano-Micro Lett.*, 2022, **15**, 26.
35. Y. Ma, D. Chen, D. D. Zhang, H. Yu, Y. P. Zheng, W. J. Li, L. Wang, Q. Liu and W. Y. Yang, *Carbon*, 2022, **187**, 196-206.
36. X. T. Zhang, Z. Y. Zhu, Y. B. Tan, K. Qin, F. X. Ma and J. H. Zhang, *Chem. Commun.*, 2021, **57**, 2049-2052.
37. R. Hao, S. Gu, J. Chen, Z. Wang, Q. Gan, Z. Wang, Y. Huang, P. Liu, K. Zhang, K. Liu, C. Liu and Z. Lu, *Mater. Today Energy*, 2021, **21**, 100826.
38. D. Wang, H. Xu, P. Yang, X. Lu, J. Ma, R. Li, L. Xiao, J. Zhang and M. An, *J. Mater. Chem. A*, 2021, **9**, 13678-13687.
39. P. Li, X. Qi, L. Zhao, J. Wang, M. Wang, M. Shao, J. S. Chen, R. Wu and Z. Wei, *J. Mater. Chem. A*, 2022, **10**, 5925-5929.
40. T. W. Wang, Q. Zhang, K. Lian, G. C. Qi, Q. Liu, L. G. Feng, G. Z. Hu, J. Luo and X. J. Liu, *J. Colloid Interface Sci.*, 2024, **655**, 176-186.
41. P. X. Weng, Y. Q. Guo, K. Wu, X. Wang, G. Q. Huang, H. Lei, Y. F. Yuan, W. G. Lu and D. Li, *J. Mater. Chem. A*, 2023, **11**, 12194-12201.
42. L. Li, N. Li, J. W. Xia, S. L. Zhou, X. Y. Qian, F. X. Yin, G. H. Dai, G. Y. He and H. Q. Chen, *Nano Res.*, 2023, **16**, 9416-9425.